Agromet 40 (1): 28-43, 2026

Agromet
journal.ipb.ac.id/index.php/agromet
ISSN : 0126 - 3633

Spatial and Temporal Drought Evaluation Based on Water Balance Using TerraClimate Data in East Java Province

Nizar Manarul Hidayat[1*], Sulistiani[2]

[1]Sub Division of Climate and Air Quality Information Production, Indonesia Agency for Meteorology Climatology and Geophysics (BMKG), Jakarta, 10110, Indonesia
[2]Climate Change Adaptation Program, KEMITRAAN (Partnership for Governance Reform), Pekalongan, 51115, Central Java, Indonesia

ARTICLE INFO

Received
21 May 2025

Revised
27 May 2026

Accepted for Publication
28 May 2026

Published
2 Jun 2026

doi: 10.29244/j.agromet.40.1.28-43

Correspondence:
Nizar Manarul Hidayat
Sub Division of Climate and Air Quality Information Production, Indonesia Agency for Meteorology Climatology and Geophysics (BMKG), Jakarta, 10110, Indonesia

Email: nizar.manarul@bmkg.go.id

ABSTRACT

Drought is one of the most critical hydrometeorological hazards affecting water resources and agricultural sustainability in East Java, Indonesia. This study evaluates the spatial and temporal characteristics of drought using a water balance approach based on TerraClimate data from 1981–2017 and validates the results against rainfall observations from 14 stations during 2008–2017. Groundwater availability (GWA) was estimated using the Thornthwaite–Mather water balance method by integrating monthly precipitation and potential evapotranspiration (PET), with adjustments for local soil properties derived from FAO soil classifications. Trend analysis using the Mann–Kendall test and Sen's slope revealed a significant increase in dry-month frequency across East Java, particularly in northern coastal and eastern regions, with trends ranging from 0.2 to 0.4 additional dry months per decade. Validation results demonstrated strong agreement between TerraClimate and observational data, with correlation coefficients ranging from 0.76 to 0.997 and RMSE values between 4.78 and 85.3 mm. Higher model performance was observed in inland and highland areas, while larger discrepancies occurred in coastal regions due to greater microclimatic variability. Seasonal analysis showed that drought conditions mainly occur from May to September, whereas water surplus periods dominate from October to March. Spatially, drought propagation was observed from northern coastal areas toward inland regions of central East Java. The findings demonstrate the reliability of TerraClimate for regional drought monitoring and support its application in early warning systems, adaptive cropping calendar management, and the development of small-scale water storage infrastructure in drought-prone areas.

KEYWORDS

drought, groundwater availability, hydrometeorology, TerraClimate, water balance

1. INTRODUCTION

Drought is one of the most complex and impactful climate-related hazards, affecting ecosystems, agriculture, water resources, and human livelihoods across the globe (Nandgude et al., 2023; Van Loon et al., 2016). Its frequency and intensity are projected to increase under climate change, particularly in tropical regions where agriculture is predominantly rainfed (Irawan et al., 2023; Spinoni et al., 2014). In Southeast Asia, drought events are strongly modulated by large-scale climate phenomena such as the El Niño–Southern Oscillation (ENSO) and the Indian Ocean Dipole (IOD), leading to high interannual variability in rainfall and prolonged dry spells (Hidayat et al., 2025).

East Java, one of Indonesia's most densely populated and agriculturally intensive provinces, is

increasingly vulnerable to drought impacts due to a combination of climatic variability, land-use change, and water demand pressures (Avia et al., 2023). Over the past decades, shifts in cropping patterns, forest degradation, and industrial growth have altered the region's hydrological balance, exacerbating water stress. Despite the growing concern, spatially explicit and long-term drought assessments in East Java remain limited in scope and resolution.

Recent advances in gridded climate data products such as TerraClimate have enabled more detailed drought assessments at regional scales. TerraClimate provides high-resolution (~4 km) monthly data on key variables like rainfall and potential evapotranspiration (Abatzoglou et al., 2018). Several global studies have successfully employed TerraClimate to detect long-term drought trends and agricultural impacts (McNally et al., 2017; Zhang et al., 2016). However, the application of TerraClimate in Indonesia, particularly for operational drought monitoring, is still underexplored. Moreover, few studies have attempted to validate TerraClimate data using ground observations in climatically diverse regions such as East Java.

To quantify drought, various indices have been developed—ranging from precipitation-only measures like the Standardized Precipitation Index (SPI) to more complex metrics incorporating evapotranspiration, such as the Standardized Precipitation Evapo-transpiration Index (SPEI) and Palmer Drought Severity Index (PDSI) (Beguería et al., 2014; Stagge et al., 2015). While these indices are widely used, they often rely on assumptions that may not suit local hydrological and agricultural systems. In this study, we adopt the Thornthwaite-Mather water balance approach, which accounts for both water input (precipitation) and demand (PET) to estimate soil moisture availability, surplus, and deficit (Thornthwaite, 1951). This method has proven effective for drought characterization in tropical climates but is rarely applied in Indonesia using high-resolution datasets.

This study seeks to address three critical knowledge gaps in the understanding of drought dynamics in East Java. First, it provides a comprehensive spatial and temporal analysis of drought conditions across the province using long-term TerraClimate data spanning the period 1981 to 2017. Second, it evaluates the accuracy of TerraClimate in estimating groundwater availability by conducting a comparative analysis with observational data derived from 14 rain gauge stations collected between 2008 and 2017. Third, it analyzes trends in the frequency and propagation of dry months by applying non-parametric statistical methods, thereby offering insights into long-term drought evolution and regional water stress patterns.

2. MATERIALS AND METHODS

2.1 Study Area

This study focuses on East Java Province (112.0–114.5 °E, 7.0–8.8 °S), featuring a tropical monsoon climate, complex topography, and diverse land use including agriculture, plantations, and urban areas. The East Java Province is situated in the eastern region of Java Island, encompassing an area of 48,033 km². The region has a population of 41,15 million people, with a population density of 857 people/km^2 (Badan Pusat Statistik, 2024). The high population density in the Java region renders it highly vulnerable to drought conditions. The incidence of meteorological drought is 15.45% higher in East Java than in Central Java (Avia et al., 2023) Over a 25-year period, East Java experienced 347 instances of drought-induced natural disasters, resulting in 1,645,587 people becoming victims and survivors. The effects of climate change also have an impact on agricultural production and food security in East Java.

2.2 Datasets

This study used monthly rainfall and potential evapotranspiration (PET) from TerraClimate at approximately 4 km spatial resolution for 1981–2017 (Abatzoglou et al., 2018). TerraClimate rainfall was evaluated using monthly observations from 14 gauge stations for 2008–2017, obtained from BMKG and local water authorities (Table 1). These observations were also used to derive station-based water availability metrics for comparison with TerraClimate-based estimates. Soil type data from FAO were used to obtain field capacity and permanent wilting point parameters required for the Thornthwaite–Mather water balance model. All datasets were processed using R Programming for spatial data processing, time-series analysis, and visualization (R Core Team, 2023). Detailed data sources are presented in Table 1.

Table 1. Types and Sources of Research Data

Type	Source	Periods
Monthly rainfall	TerraClimate Observation	1981 – 2017 2008 – 2017
Monthly PET	TerraClimate	1981 – 2017
Soil Type	FAO	-

2.3 Data Analysis

2.3.1 Potential evapotranspiration (PET) estimation

TerraClimate PET was used for province-wide gridded water-balance analysis, while station-based PET was estimated using the Thornthwaite method from nearby temperature stations for validation, as

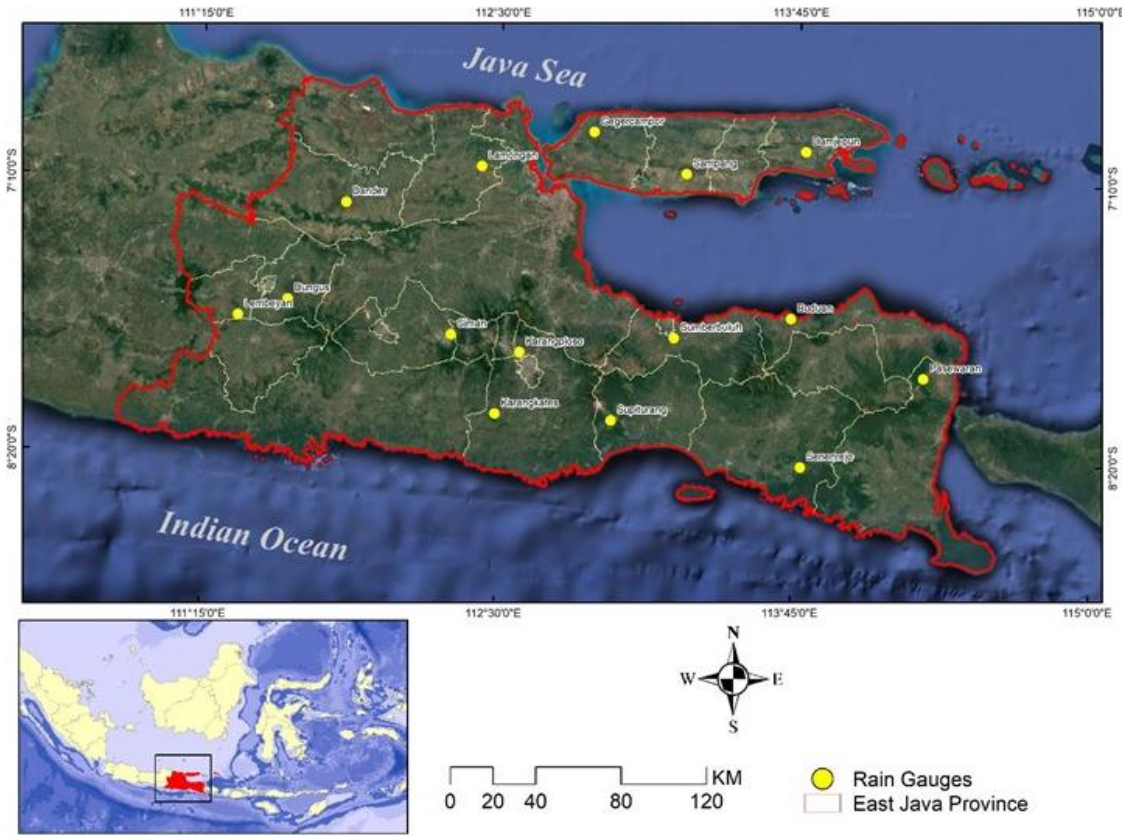

Figure 1 Study area and distribution of rain gauge stations in East Java Province, Indonesia.

direct temperature observations were unavailable at all rain gauge stations.

Potential evapotranspiration (PET) was estimated using monthly air temperature data derived from nearby reference stations. Because direct temperature observations were unavailable at most rain gauge stations, air temperature was estimated using an elevation-based lapse rate approach following Braak. Temperature interpolation employed the nearest-neighbour method, in which each rain gauge station was assigned the temperature profile of the closest reference station. Five reference stations operated by BMKG were used: Tanjung Perak, Kalianget, Pasuruan, Banyuwangi, and Yogyakarta and were grouped according to their proximity to each reference station (Table 2). Monthly PET was subsequently calculated using the Thornthwaite (Thornthwaite, 1951). PET values were used to evaluate monthly atmospheric water demand and to distinguish between surplus and deficit conditions in the water balance analysis.

2.3.2 Water balance model

The Thornthwaite–Mather water balance method was used to estimate groundwater availability (GWA) by evaluating the balance between precipitation input and evapotranspiration losses. In this study, GWA refers to climatic soil-water availability derived from the water balance system rather than directly measured groundwater storage. Therefore, it represents available water within the soil profile relevant to agricultural and climatological drought assessment.

Table 2. List of reference stations and rain gauge members in East Java

Reference Station	Associated Rain Gauge Stations
Tanjung Perak Maritime Meteorological Station	Gegercampor, Dander, Lamongan
Kalianget Meteorological Station	Damjepun, Sampang
Pasuruan Geophysical Station	Siman, Sumberbuluh, Kates
Banyuwangi Meteorological Station	Buduan, Pasewaran, Senenrejo
Yogyakarta Geophysical Station	Lembeyan, Dungus

The model was applied at a monthly timescale using precipitation (P) and potential evapotranspiration (PET) as the primary climatic inputs. Drought conditions develop when precipitation is insufficient to meet atmospheric water demand (PET), leading to progressive depletion of soil water storage. The model also incorporates soil water holding capacity through field capacity (FC) and permanent wilting point (PWP), which regulate the amount of water that can be stored and released by the soil.

The analysis began by calculating the difference between precipitation and PET (P − PET). When precipitation exceeded PET, no water deficit accumulated and the Accumulated Potential Water Loss (APWL) was set to zero. Conversely, when precipitation was lower than PET, APWL was calculated as the cumulative deficit. Soil Water Content (SWC) was estimated based on field capacity (FC) and APWL. Under water-deficit conditions, SWC was calculated using Equation 1.

$$SWC = FC \times e^{\left(\frac{APWL}{-FC}\right)} \quad (1)$$

When precipitation exceeded PET, the soil was assumed to be fully replenished and SWC was equal to FC. Field Capacity (FC) and Permanent Wilting Point (PWP) were derived from FAO-based soil classifications and converted into gridded spatial layers. For mineral soils in East Java, FC and PWP were generally assumed to be approximately 125 mm and 50 mm, respectively.

Actual evapotranspiration (ETA) was then estimated according to moisture conditions. When precipitation exceeded PET, ETA was assumed equal to PET. Under deficit conditions, ETA was calculated using Equation 2, where ΔSWC represents the monthly change in soil water content.

$$ETA = P - \Delta SWC \quad (2)$$

Water deficit (D) and surplus (S) were subsequently determined using Equations (3) and (4), respectively: Drought severity was quantified using the Thornthwaite–Mather drought index, expressed as the percentage ratio between water deficit and PET using Equation (5).

$$D = PET - ETA \quad (3)$$
$$S = (P - PET) - \Delta SWC \quad (4)$$
$$I_a = 100 \times \frac{D}{PET} \quad (5)$$

where I_a is the drought index, D is water deficit, and PET is potential evapotranspiration. The drought index was classified into three categories: mild drought (0–16.7%), moderate drought (16.7–33.3%), and severe drought (>33.3%).

2.3.3 Trend Analysis

Trends in dry-month frequency were analyzed using the non-parametric Mann–Kendall (MK) test, which has been widely applied to detect temporal changes in hydroclimatic conditions (Ahmadi et al., 2018; Hidayat et al., 2025). The MK test is commonly used in climatological studies because it is robust against outliers and does not require normally distributed data (Jiang et al., 2019; Onyutha, 2016). This characteristic makes it particularly suitable for tropical regions such as East Java, where rainfall exhibits high spatial and temporal variability.

A dry month was defined as a month with precipitation below 60 mm for each grid cell during the 1981–2017 period, following the dry-month threshold used in the Köppen–Geiger tropical climate classification and the Schmidt–Ferguson/Mohr agroclimatic classification commonly applied in Indonesia (Kottek et al., 2006). The annual number of dry months was then calculated and analyzed using the Mann–Kendall test at a 95% confidence level. Trends were considered statistically significant when the standardized z-value exceeded ±1.96 ($p < 0.05$). All analyses were performed using the R programming language. The trend package was used for trend analysis (Pohlert, 2023), while tidyverse and ggplot2 were used for data processing and visualization (Wickham et al., 2019).

3. RESULTS AND DISCUSSION

3.1 Seasonal rainfall

Figure 2 presents an analysis of seasonal rainfall using TerraClimate satellite data. Based on 37 years of TerraClimate data, the total precipitation during the December-January-February (DJF) period is the highest compared to other seasonal periods. The regions experiencing the highest rainfall are central and parts of western East Java, including Malang Regency, Kediri, Batu City, Lumajang Regency, Bondowoso, and Situbondo. In contrast, the period with the lowest precipitation is June-July-August (JJA). During this time, most of the northern coastal areas of East Java experience a total rainfall of only 0 – 50 mm. These two seasonal periods indicate the peaks of the rainy and dry seasons, with the rainy season peaking during DJF and the dry season during JJA (Harijanto et al., 2012).

Meanwhile, the March-April-May (MAM) and September-October-November (SON) periods are characterized by transitional periods from the rainy to the dry season. Rainfall patterns derived from TerraClimate data also exhibit distinct characteristics in the central to southern regions of East Java, which experience higher precipitation. In contrast, lower rainfall is observed in the northern regions of East Java. The rainfall distribution in East Java is closely related to elevation levels, where areas with higher topography exhibit orographic effects, contributing to increased slope rainfall (Giarno et al., 2020).

As derived from land water balance calculations, the spatial distribution of monthly water deficits provides valuable insights into regional hydrological dynamics. This analysis reveals how water deficits vary

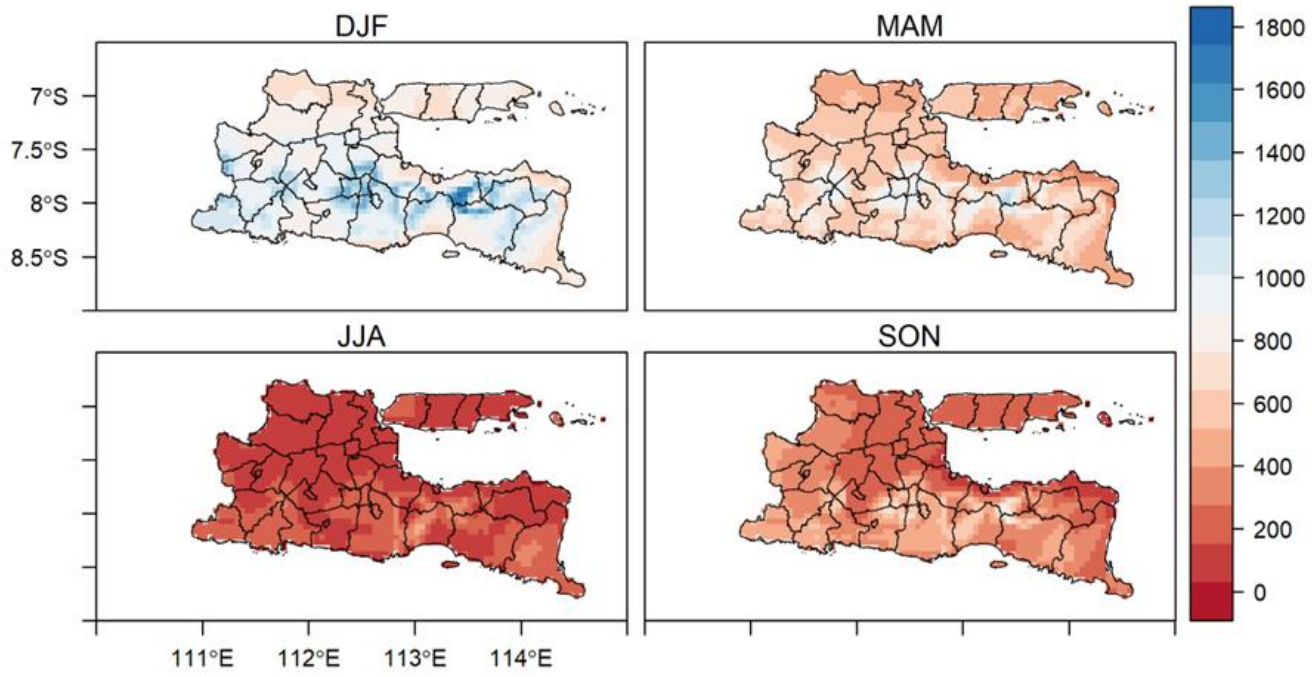

Figure 2. Spatial distribution of seasonal rainfall accumulation (mm) based on TerraClimate data for 1981–2017.

across different areas, influenced by climatic factors and land use patterns. Typically, the findings indicate that certain regions experience more significant water deficits during specific months, often correlating with seasonal changes in rainfall and temperature. For instance, deficits may peak during the dry season, particularly in June, July, and August, while showing recovery during the rainy season, especially from November to March.

Calculating the land water balance yields monthly estimates of water deficits and surpluses. Most regions in East Java begin to experience water deficits starting in May, with values ranging from 0 to 40 mm. This water deficit condition expands as the dry season progresses, particularly during the peak of the dry season in July and August. This period, known as the June-July-August (JJA) season, as shown in Figure 3, marks the height of the dry season, resulting in widespread drought across East Java. The northern areas, including Situbondo, Probolinggo, Surabaya, Tuban, and Madura Island, are particularly affected by prolonged drought conditions. These regions also have higher population densities than the southern areas, leading to increased water usage and further intensifying the impact of water scarcity (Avia et al., 2023). However, the water deficit begins to subside by October as the transition from the dry to the rainy season occurs. Maps illustrating the spatial distribution of monthly water deficits can highlight critical areas that require attention for water resource management, agricultural planning, and drought mitigation strategies.

Understanding the spatial distribution of monthly water surpluses, particularly groundwater availability, is essential for effective water resource management in East Java, where groundwater supports agriculture, domestic needs, and industrial activities. The results indicate that water surpluses increase during the rainy season, especially from November to February (Figure 2). Areas with high groundwater recharge generally correspond to regions with higher rainfall, reflecting effective water infiltration and storage. Surpluses typically begin in October over central East Java and intensify during the November–February period, reaching approximately 300–600 mm (Figure A1). The highest surpluses occur in Ngawi, Nganjuk, Malang, Lumajang, and Jember, mainly due to orographic rainfall enhancement associated with mountainous regions such as Bromo, Semeru, Kelud-Kawi, Lawu, Ngliman, and Raung.

Groundwater availability in East Java is primarily influenced by rainfall patterns, land use, soil properties, and topography. The region experiences a distinct wet season from October to April and a dry season from May to September, making rainfall variability a key factor controlling groundwater recharge. Land use and land cover (LULC) also strongly affect water availability. Urbanization increases impervious surfaces, leading to greater surface runoff and reduced infiltration capacity (Weatherl et al., 2021). In addition, hydrological characteristics such as soil type and topography influence infiltration and water storage processes (Sujarwo et al., 2019). Areas with porous soils and gentle slopes generally promote higher groundwater recharge compared to steep or compacted landscapes.

Spatial distribution insights at along the northern coast, including areas like Situbondo and Probolinggo,

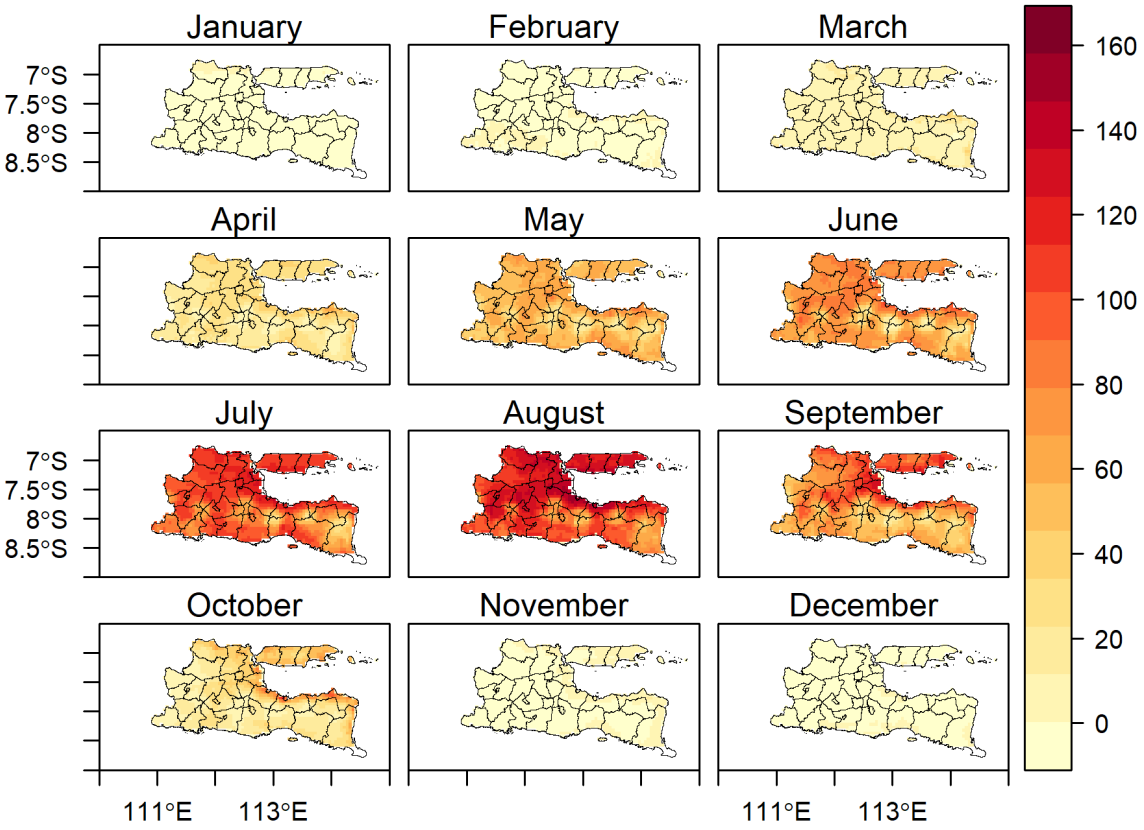

Figure 3. Spatial distribution of climatological monthly water deficit (D, mm month^{-1}) estimated using the Thornthwaite–Mather water balance model for 1981–2017.

often face water deficits during the dry season due to lower rainfall and higher evaporation. These areas may experience reduced groundwater levels, leading to potential shortages. While, central east Java such as Ngawi, Nganjuk, and Malang typically exhibit higher groundwater availability. This is attributed to favorable rainfall patterns and soil conditions that promote effective recharge. Finally at areas in the south, like Lumajang and Jember, benefit from higher rainfall and abundant groundwater resources. However, they may also face challenges related to land use changes, which can impact water availability. Groundwater levels fluctuate seasonally, with surpluses often observed during the wet season (November to February) when rainfall exceeds evapotranspiration. Conversely, deficits are more common during the dry season (May to September) when evapotranspiration surpasses rainfall.

The spatial distribution of the monthly Thornthwaite-Mather Drought Index provides a comprehensive overview of drought conditions across a specific region (Figure 4). The index often shows heightened drought levels during the dry season, particularly from June to August, reflecting reduced rainfall and increased evapotranspiration rates. During this period, regions in the northern coastal areas and parts of the central region may exhibit severe drought conditions. As the rainy season approaches, the drought index may begin to decrease from September to October, indicating a transition from dry to wetter conditions. However, some areas may still show signs of light drought, particularly in locations where rainfall is less abundant. Mountainous areas receive more precipitation than low-lying coastal regions due to orographic lifting, which enhances rainfall as moist air ascends over mountains (Kim et al., 2022).

Early signs of drought are observed in March, particularly in the northern coastal regions, such as Situbondo and Banyuwangi. By April, drought indications become more pronounced in these northern coastal areas and intensify through May. The peak of the dry season, occurring during the June-July-August period, results in widespread and severe drought conditions across East Java. The intensity and extent of the drought gradually decrease as rainfall begins to occur in parts of East Java. By October, drought conditions continue to decline as the region transitions into the rainy season. However, northern coastal areas and Madura Island still experience drought, even as the rainy season stabilizes in November. Light drought conditions persist in the northern coastal region, Madura Island, and Banyuwangi despite the onset of consistent rainfall during the rainy season.

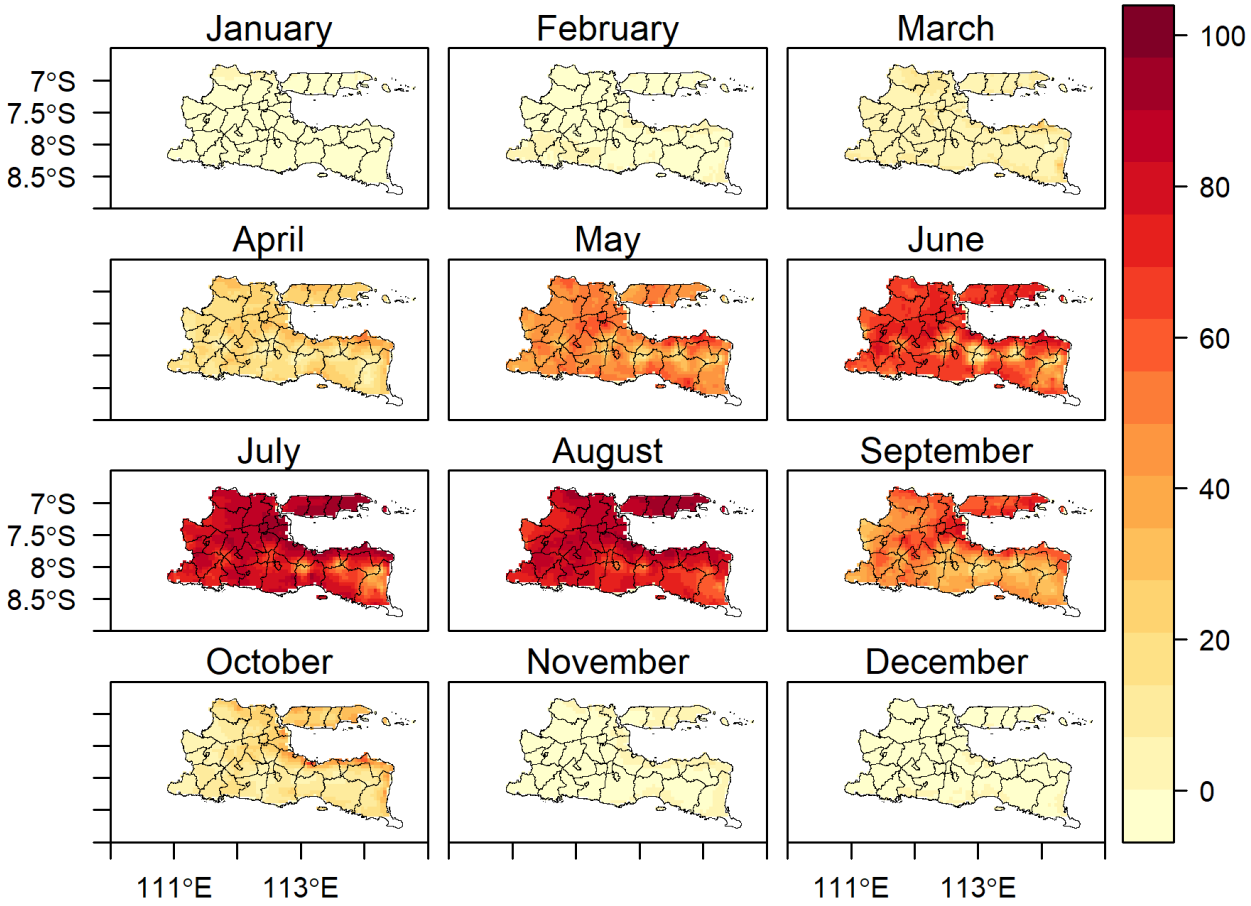

Figure 4. Spatial Distribution of Monthly Thornthwaite–Mather Drought Index (%)

The Thornthwaite–Mather drought index shown in Figure 4 is expressed as a percentage, representing the proportion of potential evapotranspiration that cannot be fulfilled by available water. Higher percentage values indicate a larger water deficit relative to atmospheric water demand, and therefore represent drier or more severe drought conditions.

This suggests that drought propagation typically begins in the northern coastal regions, with light drought emerging as early as April and increasing to more than 33.3% by August. In September, drought conditions begin to recede in most areas, with further relief by October. Maps illustrating the spatial distribution of monthly water deficits can highlight critical areas that require attention for water resource management, agricultural planning, and drought mitigation strategies (Cavus and Aksoy, 2019). By identifying regions that consistently exhibit higher deficits, policymakers can allocate resources more effectively and implement targeted interventions to enhance water availability and resilience against drought (Apurv and Cai, 2020).

These findings resonate with drought progression patterns observed in other dryland regions globally. For instance, identified similar early season drought signals and intensification in semi-arid Turkey, emphasizing the role of topography and landuse interactions in amplifying drought severity (Cavus and Aksoy, 2019). Likewise, observed that in African dryland zones, delayed rainfall onset and weak soil moisture retention played key roles in the severity of agricultural droughts (Christian et al., 2021). While east Java experiences a monsoonal tropical climate, the northern coastal zones and madura Island display behavioral similarities with these regions in terms of vulnerability and seasonal dryness. Situating East Java's drought dynamics within this broader global narrative provides valuable insights for designing cross-context drought mitigation strategies and enhances the international relevance of this study.

3.2 Dry months duration trend

The map indicates several regions with a significant increase in dry months, highlighted in deep red, as shown in Figure 5. These areas are primarily located in northern and central parts of East Java, which have consistently experienced prolonged dry conditions over the observed period. Areas shaded in lighter red indicate regions where dry month durations have increased but not to a statistically significant extent. These areas might still face challenges related to water scarcity but are less severely affected than

those marked as "Significantly Down." The map showcases variability within East Java, where some districts exhibit significant trends towards increased dry month durations while others remain relatively stable. This spatial heterogeneity suggests that local topography, land-use patterns, and microclimatic factors play crucial roles in modulating regional drought dynamics. In mountainous terrain, orographic effects can substantially influence rainfall distribution, often creating distinct rain-shadow zones that exacerbate dryness in adjacent lowlands (As-syakur et al., 2016; Hidayat and Taufik, 2025).

The analysis shows that coastal regions, particularly in the northern part of East Java, experience longer dry periods compared to some inland areas, suggesting that maritime influences may affect local rainfall patterns. Generally, regions experiencing drought duration trends are predominantly located in central to southern East Java, with smaller areas in the northern and western parts of the province. TerraClimate data over the past 37 years indicate a significant increase in drought occurrences across East Java. This upward trend in drought duration highlights the region's growing vulnerability, particularly in areas with already arid conditions, further exacerbating water scarcity challenges. The identified dry regions, particularly those with significant upward trends in dry month durations, are likely more vulnerable to water resource challenges. Northern coastal districts and certain central regions should be prioritized for water management interventions. Analyzing the spatial distribution of dry month duration trends reveals critical insights into regional drought patterns and variability (Christian et al., 2021)**.** This information is essential for informing effective water management strategies and adaptive measures to address potential future water scarcity issues in East Java.

3.3 Comparison of Monthly Groundwater Availability

Both monthly groundwater availability values and data from TerraClimate show a similar pattern as shown in Figure A2, particularly from December to May. In many regions, there is a decrease in groundwater availability values during the June to October period. Despite November marking the start of the rainy season, certain areas such as Lamongan, Buduan, and Pasewaran exhibit groundwater availability values below the threshold limit for soil moisture (TLP). This indicates that even with the onset of rains, soil moisture recovery in these areas remains insufficient, suggesting localized challenges in replenishing soil water content. Both observational data and TerraClimate datasets may show similar patterns in monthly groundwater availability values, particularly during peak rainy months (December to February) and dry months (June to August). This suggests that TerraClimate effectively captures significant seasonal variations in groundwater availability. Nevertheless, minor discrepancies between the two datasets can occur during transitional periods, such as March and November, where differences in rainfall estimates subsequently drive variations in groundwater availability.

3.4 Performance Evaluation of TerraClimate-Derived KAT using Observed Data

The validation compares TerraClimate-derived water-balance estimates with station-based water-balance estimates derived from observed rainfall, rather than direct groundwater measurements. Based on the evaluation metrics Table A1, Sumberpuluh, Pasewaran, and Siman stations demonstrated the lowest Mean Absolute Error (MAE) and Root Mean Square Error (RMSE), with correlation coefficients exceeding 0.99. These results indicate that the TerraClimate model performs exceptionally well in capturing the temporal variability of Groundwater Availability (KAT) at these locations. The high correlation values, which are close to 1, suggest that the seasonal fluctuation patterns from the model are highly consistent with observational data. Overall, approximately half of the stations exhibit MAE values below 20 mm and correlation coefficients above 0.99, reflecting accurate and reliable estimation performance across the region.

Conversely, several stations such as Sampang, Dander, and Bangkalan show relatively high error values, with MAE exceeding 30 mm and correlation coefficients below 0.80. This implies a substantial deviation between the model outputs and observed data, which may be attributed to local heterogeneity not adequately captured by the spatial resolution of TerraClimate or limitations in the input datasets in those areas. These findings highlight the importance of localized validation and spatial model adjustments, particularly in hydrologically and topographically complex regions (Hidayat and Taufik, 2025). Therefore, the application of TerraClimate in areas with lower performance should be accompanied by bias correction approaches or the integration of local datasets to enhance the representativeness of KAT estimations.

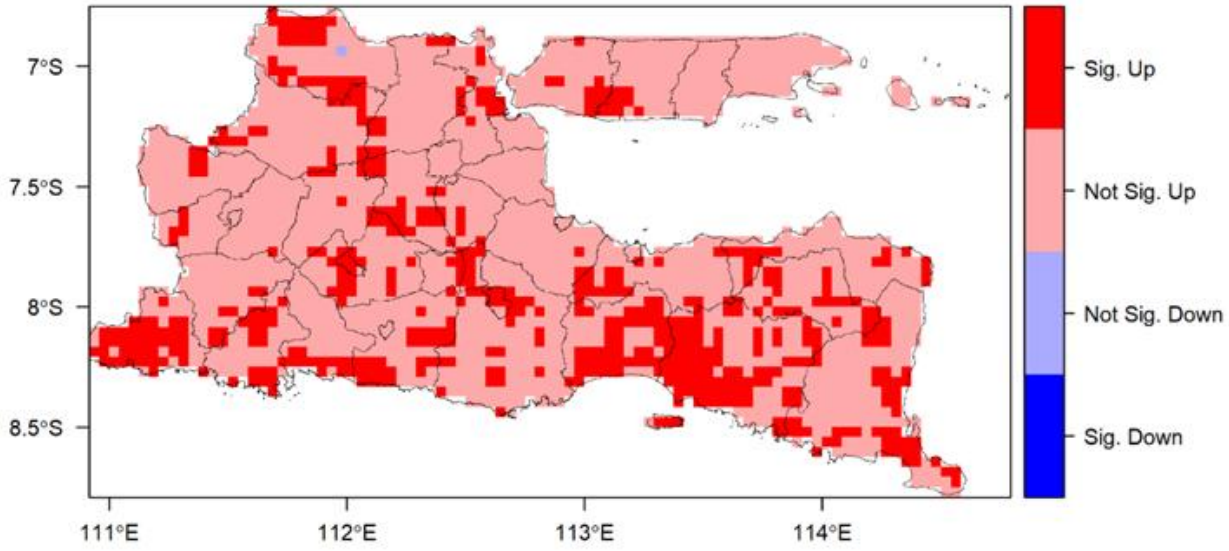

Figure 5. Spatial Distribution Map of Dry Month Duration Trends over 37 Years

Validation of TerraClimate-derived groundwater availability (GWA) against station-based estimates from 14 rain gauge locations across East Java during 2008–2017 reveals a generally strong agreement, though spatial variability in performance is evident. The Pearson correlation coefficients range from 0.762 to 0.997, indicating that TerraClimate effectively captures temporal fluctuations in GWA, particularly in inland and highland areas such as Sumberpulo, Pasewaran, Siman, and Karangploso, where correlations exceed 0.99 and root mean square errors (RMSE) remain below 13.5 mm. These locations exhibit minimal bias, with mean absolute errors (MAE) under 7.5 mm, reflecting the robustness of TerraClimate in regions with stable orographic and hydrological conditions.

In contrast, stations located in more coastal or heterogeneous environments—such as Sampang (r = 0.77, RMSE = 83 mm) and Dander (r = 0.76, RMSE = 85 mm)—demonstrate lower predictive performance, with larger deviations likely attributable to localized microclimatic effects, coastal convection variability, or mismatches between gridded TerraClimate resolution and the fine-scale characteristics of these regions. The Taylor diagram further supports this assessment, showing that these lower-performing stations deviate more substantially in terms of both correlation and standard deviation when compared to others. The range of RMSE values, from as low as 4.78 mm at Sumberpulo to over 85 mm at Dander, highlights the importance of spatial context in interpreting gridded climate data performance. Notably, the best-performing stations are not uniformly distributed, suggesting that topography, land use, and proximity to reference meteorological stations used in the PET estimation process may also influence model accuracy. These findings suggest that while TerraClimate offers reliable estimates for most regions in East Java, caution is warranted when interpreting results in low-performing areas. The discrepancies emphasize the importance of integrating local calibration or supplemental station data in such zones to improve accuracy in future applications, especially when used for operational drought monitoring or water management decisions.

The Taylor diagram provides a comprehensive evaluation of TerraClimate performance by simultaneously comparing correlation, standard deviation, and centered RMSE (Figure 6). Stations such as Pasewaran and Sumberbuluh are positioned close to the reference point, indicating high correlation, low RMSE, and variability comparable to observations. This suggests that TerraClimate effectively captures the seasonal dynamics of groundwater availability in these regions. In contrast, stations such as Dander and Sampang show lower agreement, reflected by lower correlation and greater deviations in standard deviation and RMSE, likely due to local climatic variability and the coarse spatial resolution of the dataset. Overall, inland and highland areas exhibit better model performance than coastal and transitional regions, indicating that TerraClimate is more reliable in areas with relatively uniform climatological conditions. Despite some limitations in complex coastal environments, TerraClimate performs satisfactorily across most stations in East Java and is suitable for regional drought and groundwater assessments.

Our analysis of groundwater availability (GWA) across East Java highlights a clear seasonal deficit pattern, with May to September characterized by the most pronounced dry spells. Spatially, the northern coastal zone consistently exhibits earlier onset and prolonged drought conditions compared to central

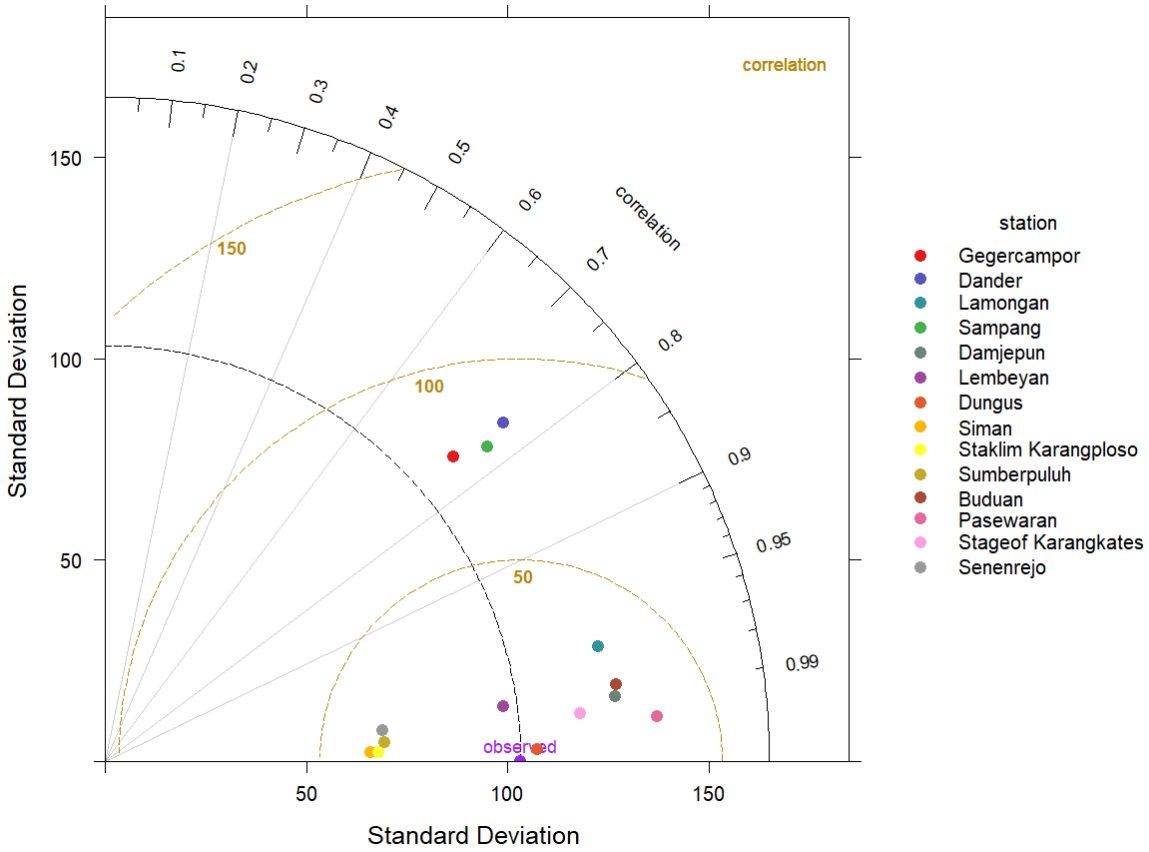

Figure 6. Taylor Diagram for GWA Evaluation at 14 Meteorological Stations in East Java

and southern inland areas, which can be attributed to its lower rainfall input combined with higher evapotranspiration rates driven by landscape and land-use characteristics.

Trend analysis using the Mann–Kendall test revealed a statistically significant increase in the number of dry months (GWA < 0) per year ($z > 1.96$; $p < 0.05$), with Sen's slope estimations indicating a rise of 0.2–0.4 dry months per decade. Spatially, the significance map (Figure Y) illustrates widespread intenssification of drought frequency, with over 35% of the province showing significant upward trends, particularly concentrated in the northern, eastern, and southern fringes of East Java. The spatial clustering of statistically significant trends in these zones highlights areas of heightened vulnerability, which aligns with broader climatological observations indicating an expansion of seasonal aridity in tropical maritime regions.

Practical implications emerge clearly from these findings. Given the early and extended drought conditions in the northern coastal zone, the construction of embung (small artificial reservoirs) is recommended to enhance local water storage capacity during the wet season, ensuring reliable supplementary water supplies in the dry months. This approach aligns with positive outcomes documented in other Indonesian regions where embung has successfully buffered agricultural production and supported ecosystem resilience. Additionally, our findings support the need for a strategic shift in cropping calendars, especially for rainfed rice in the northern zone; advancing planting toward the onset of the wet season or switching to more drought-resilient crops could reduce exposure to peak deficits. This aligns with adaptive agricultural strategies prioritized in national drought management frameworks.

Nevertheless, caution is warranted when applying these strategies: TerraClimate's sigma performance in coastal microclimates and assumptions of homogeneous soil properties in water balance calculations necessitate site-specific feasibility studies. Meanwhile, embung design and implementation must account for local geology, hydrology, and community involvement to ensure long-term effectiveness.

Despite these limitations, the convergence of TerraClimate-based GWA estimates and ground observations, combined with pronounced spatial trends and clear seasonal drought dynamics, supports targeted interventions such as water retention infrastructure and cropping calendar adjustments. These measures, backed by quantifiable data and robust statistical validation, provide a strong foundation for early-warning systems and informed water-management strategies tailored to provincial and local needs.

Observational data often indicate higher GWA values in regions where local groundwater recharge is enhanced by microclimatic precipitation patterns. TerraClimate might show peaks reflecting broader regional trends rather than localized conditions, potentially missing specific microclimatic effects in the observational data. During dry months, observational data may reveal lower groundwater availability values in areas particularly vulnerable to drought. TerraClimate might average these effects across larger areas, leading to less pronounced reductions in groundwater availability.

The comparative analysis of monthly GWA values derived from observational data and TerraClimate underscores the critical importance of integrating multi-source datasets for comprehensive groundwater management. While TerraClimate offers valuable insights into macro-regional patterns, observational data provide the indispensable local context required for site-specific precision. Continuous evaluation and calibration of these datasets will enhance their reliability and usefulness in addressing water resource challenges. Understanding the differences and similarities between observational and TerraClimate groundwater avail-ability values is crucial for water resource management. Policymakers can utilize both datasets to formulate strategies that consider both ground conditions and broader climatic patterns and trends, ensuring more effective and sustainable water use (Amanambu et al., 2020).

4. CONCLUSION

This study reveals that drought in East Java over the past 37 years tends to occur earlier and more intensely, particularly in the northern coastal region, Madura Island, and parts of the central inland area. The dry season typically begins in April and peaks between June and August, marked by an increasing number of dry months and greater water deficits. TerraClimate data showed strong agreement with observed soil moisture in most regions, although significant discrepancies were found in highland areas such as Malang and Ponorogo.

This study acknowledges several limitations, including the 4-km spatial resolution of TerraClimate, generalized soil hydraulic parameters, and simplified PET estimation within the Thornthwaite–Mather framework. The validation was conducted against station-based water-balance estimates rather than direct groundwater measurements. Therefore, the results are most suitable for regional drought monitoring and prioritization, while local-scale implementation should be supported by field hydrological observations, land-use information, and bias correction in lower-performing coastal areas.

These finding can inform adaptive drought mitigation and water resource management policies, especially in high-risk areas. Local governments are encouraged to strengthen early warning systems, implement dry season-based irrigation planning, and enhance water infrastructure management. This study acknowledges limitations related to the coarse spatial resolution of satellite data and simplified assumptions within the Thornthwaite-Mather method. Future research should integrate socio-economic vulnerability indicators, dynamic land use patterns, and machine learning models to improve drought monitoring and decision making in tropical regions.

ACKNOWLEDGEMENT

In this study, we thank the Karangploso Climatology Station for providing rainfall data and rain gauge station information, complete with elevation data. We also extend our sincere gratitude to the research team for their contributions in processing the observational data and for offering valuable insights and suggestions, both directly and indirectly, throughout the course of this work. Their support has been instrumental in the successful completion of this analysis.

REFERENCES

Abatzoglou, J.T., Dobrowski, S.Z., Parks, S.A., Hegewisch, K.C., 2018. TerraClimate, a high-resolution global dataset of monthly climate and climatic water balance from 1958–2015. Sci Data 5, 170191. https://doi.org/10.1038/sdata.2017.191

Ahmadi, F., Nazeri Tahroudi, M., Mirabbasi, R., Khalili, K., Jhajharia, D., 2018. Spatiotemporal trend and abrupt change analysis of temperature in Iran. Meteorological Applications 25, 314–321.

Amanambu, A.C., Obarein, O.A., Mossa, J., Li, L., Ayeni, S.S., Balogun, O., Oyebamiji, A., Ochege, F.U., 2020. Groundwater system and climate change: Present status and future considerations. Journal of Hydrology 589, 125163. https://doi.org/10.1016/j.jhydrol.2020.125163

Apurv, T., Cai, X., 2020. Impact of Droughts on Water Supply in U.S. Watersheds: The Role of Renewable Surface and Groundwater Resources. Earth's Future 8, e2020EF001648. https://doi.org/10.1029/2020EF001648

As-syakur, A.R., Osawa, T., Miura, F., Nuarsa, I.W., Ekayanti, N.W., Dharma, I.G.B.S., Adnyana, I.W.S., Arthana, I.W., Tanaka, T., 2016. Maritime Continent rainfall variability during the TRMM era: The role of monsoon, topography and El Niño Modoki. Dynamics of Atmospheres and Oceans 75, 58–77.

Avia, L.Q., Yulihastin, E., Izzaturrahim, M.H., Muharsyah, R., Satyawardhana, H., Sofiati, I., Nurfindarti, E. Gammamerdianti, 2023. The spatial distribution of a comprehensive drought risk index in Java, Indonesia. Kuwait Journal of Science 50, 753–760. https://doi.org/10.1016/j.kjs.2023.02.031

Badan Pusat Statistik, 2024. Provinsi Jawa Timur Dalam Angka. BPS Provinsi Jawa Timur.

Beguería, S., Vicente-Serrano, S.M., Reig, F., Latorre, B., 2014. Standardized precipitation evapotranspiration index (SPEI) revisited: parameter fitting, evapotranspiration models, tools, datasets and drought monitoring. Int. J. Climatol. 34, 3001–3023. https://doi.org/10.1002/joc.3887

Cavus, Y., Aksoy, H., 2019. Spatial Drought Characterization for Seyhan River Basin in the Mediterranean Region of Turkey. Water 11, 1331. https://doi.org/10.3390/w11071331

Christian, J.I., Basara, J.B., Hunt, E.D., Otkin, J.A., Furtado, J.C., Mishra, V., Xiao, X., Randall, R.M., 2021. Global distribution, trends, and drivers of flash drought occurrence. Nat Commun 12, 6330. https://doi.org/10.1038/s41467-021-26692-z

Giarno, Hadi, M.P., Suprayogi, S., Herumurti, S., 2020. Impact of rainfall intensity, monsoon and MJO to rainfall merging in the Indonesian maritime continent. J Earth Syst Sci 129, 164. https://doi.org/10.1007/s12040-020-01427-8

Harijanto, F.D., Kuntjoro, K., Saptarita, S., Aziz, S.K., 2012. Analisis Pola Hujan dan Musim di Jawa Timur Sebagai Langkah Awal Untuk Antisipasi Bencana Kekeringan. JITS 10, 95. https://doi.org/10.12962/j12345678.v10i2.2672

Hidayat, R., Apip, Dasril, A.P., Taufik, M., 2025. Climate teleconnection triggers prolonged dry season in tropical maritime continent. Theor Appl Climatol 156, 626. https://doi.org/10.1007/s00704-025-05852-x

Hidayat, R., Taufik, M., 2025. Bias Correction of CMIP6 Models for Assessment of Wet and Dry Conditions Over Sumatra. Agromet 39, 33–39. https://doi.org/10.29244/j.agromet.39.1.33-39

Irawan, A.N.R., Komori, D., Hendrawan, V.S.A., 2023. Correlation analysis of agricultural drought risk on wet farming crop and meteorological drought index in the tropical-humid region. Theor Appl Climatol 153, 227–240. https://doi.org/10.1007/s00704-023-04461-w

Jiang, Y., Zhou, L., Tucker, C.J., Raghavendra, A., Hua, W., Liu, Y.Y., Joiner, J., 2019. Widespread increase of boreal summer dry season length over the Congo rainforest. Nat. Clim. Chang. 9, 617–622. https://doi.org/10.1038/s41558-019-0512-y

Kim, H.-J., Jung, W., Suh, S.-H., Lee, D.-I., You, C.-H., 2022. The Characteristics of Raindrop Size Distribution at Windward and Leeward Side over Mountain Area. Remote Sensing 14, 2419. https://doi.org/10.3390/rs14102419

Kottek, M., Grieser, J., Beck, C., Rudolf, B., Rubel, F., 2006. World Map of the Köppen-Geiger climate classification updated. Meteorologische Zeitschrift 15, 259–263. https://doi.org/10.1127/0941-2948/2006/0130

McNally, A., Arsenault, K., Kumar, S., Shukla, S., Peterson, P., Wang, S., Funk, C., Peters-Lidard, C.D., Verdin, J.P., 2017. A land data assimilation system for sub-Saharan Africa food and water security applications. Sci Data 4, 170012. https://doi.org/10.1038/sdata.2017.12

Nandgude, N., Singh, T.P., Nandgude, S., Tiwari, M., 2023. Drought Prediction: A Comprehensive Review of Different Drought Prediction Models and Adopted Technologies. Sustainability 15, 11684. https://doi.org/10.3390/su151511684

Onyutha, C., 2016. Identification of sub-trends from hydro-meteorological series. Stochastic environmental research and risk assessment 30, 189–205.

Pohlert, T., 2023. trend: Non-Parametric Trend Tests and Change-Point Detection.

R Core Team, 2023. R: A language and environment for statistical computing.

Spinoni, J., Naumann, G., Carrao, H., Barbosa, P., Vogt, J., 2014. World drought frequency, duration, and severity for 1951-2010: WORLD DROUGHT CLIMATOLOGIES FOR 1951-2010. Int. J. Climatol. 34, 2792–2804. https://doi.org/10.1002/joc.3875

Stagge, J.H., Tallaksen, L.M., Gudmundsson, L., Van Loon, A.F., Stahl, K., 2015. Candidate Distributions for Climatological Drought Indices (SPI and SPEI). Intl Journal of Climatology 35, 4027–4040. https://doi.org/10.1002/joc.4267

Sujarwo, M.W., Indarto, I., Wiratama, E., Teguh, B., 2019. Assesment of morphometric and hydrological properties of smalls watersheds in East Java Regions. JTS ITB 26, 97–110. https://doi.org/10.5614/jts.2019.26.2.2

Thornthwaite, C.W., 1951. The Water Balance in Tropical Climates. Bulletin of the American Meteorological Society 32, 166–173. https://doi.org/10.1175/1520-0477-32.5.166

Van Loon, A.F., Gleeson, T., Clark, J., Van Dijk, A.I.J.M., Stahl, K., Hannaford, J., Di Baldassarre, G., Teuling, A.J., Tallaksen, L.M., Uijlenhoet, R., Hannah, D.M., Sheffield, J., Svoboda, M., Verbeiren, B., Wagener, T., Rangecroft, S., Wanders, N., Van Lanen, H.A.J., 2016. Drought in the Anthropocene. Nature

Geosci 9, 89–91. https://doi.org/10.1038/ngeo2646

Weatherl, R.K., Henao Salgado, M.J., Ramgraber, M., Moeck, C., Schirmer, M., 2021. Estimating surface runoff and groundwater recharge in an urban catchment using a water balance approach. Hydrogeol J 29, 2411–2428. https://doi.org/10.1007/s10040-021-02385-1

Wickham, H., Averick, M., Bryan, J., Chang, W., McGowan, L., François, R., Grolemund, G., Hayes, A., Henry, L., Hester, J., Kuhn, M., Pedersen, T., Miller, E., Bache, S., Müller, K., Ooms, J., Robinson, D., Seidel, D., Spinu, V., Takahashi, K., Vaughan, D., Wilke, C., Woo, K., Yutani, H., 2019. Welcome to the Tidyverse. JOSS 4, 1686. https://doi.org/10.21105/joss.01686

Zhang, Y., Peng, C., Li, W., Tian, L., Zhu, Q., Chen, H., Fang, X., Zhang, G., Liu, G., Mu, X., Li, Z., Li, S., Yang, Y., Wang, J., Xiao, X., 2016. Multiple afforestation programs accelerate the greenness in the 'Three North' region of China from 1982 to 2013. Ecological Indicators 61, 404–412. https://doi.org/10.1016/j.ecolind.2015.09.041

ANNEX

Table A1 Performance Evaluation of TerraClimate-Derived KAT Using Observed Data

Station	MAE	RMSE	Correlation	Rank MAE
Sumberpuluh	2.54	4.78	0.997	1
Pasewaran	6.35	11.23	0.996	2
Siman	7.17	12.35	0.999	3
Staklim Karangploso	7.65	13.25	0.999	4
Dungus	7.73	11.87	0.999	5
Damjepun	11.24	18.53	0.992	6
Stageof Karangkates	15.27	21.84	0.995	7
Senenrejo	16.55	28.21	0.994	8
Buduan	18.24	23.46	0.988	9
Lembeyan	24.68	39.68	0.990	10
Lamongan	27.25652	36.59394	0.974038	11
Gegercampor	33.42932	80.39934	0.753023	12
Dander	33.85604	85.26734	0.762254	13
Sampang	36.71759	83.0059	0.772735	14

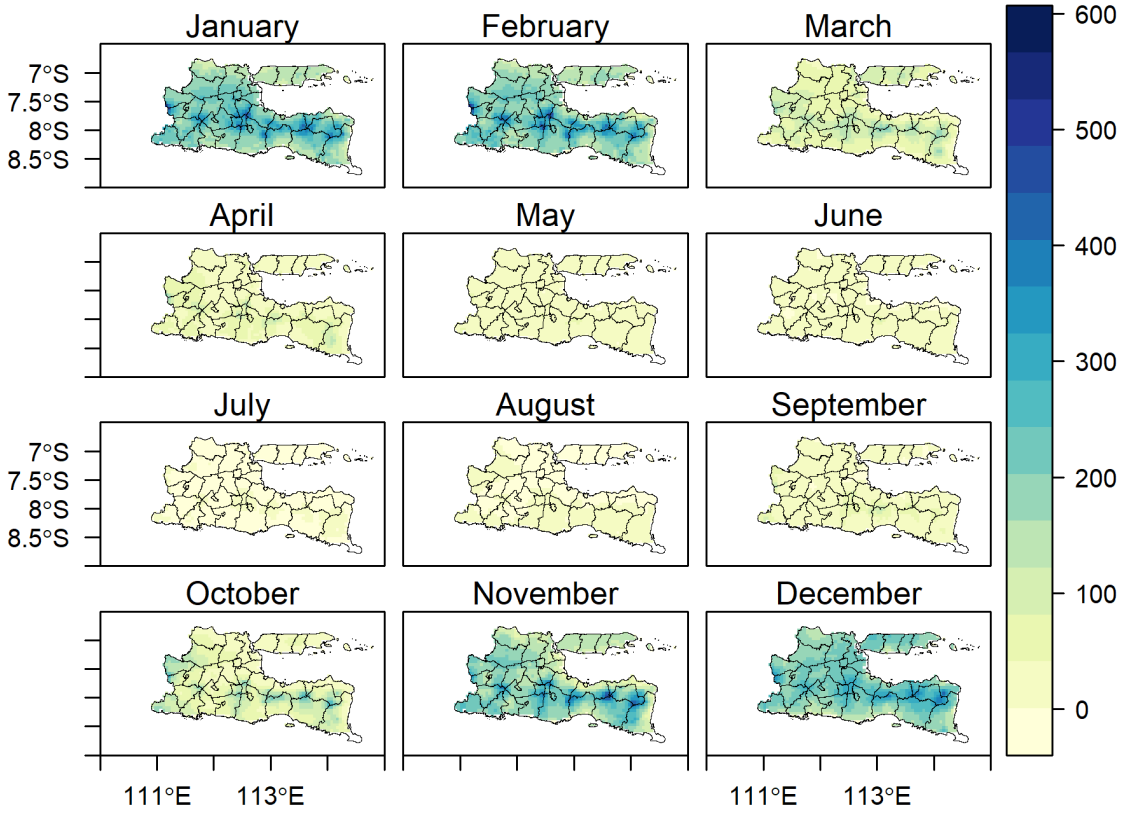

Figure A1. Spatial Distribution of Monthly Water Surplus Based on Groundwater Availability Calculations

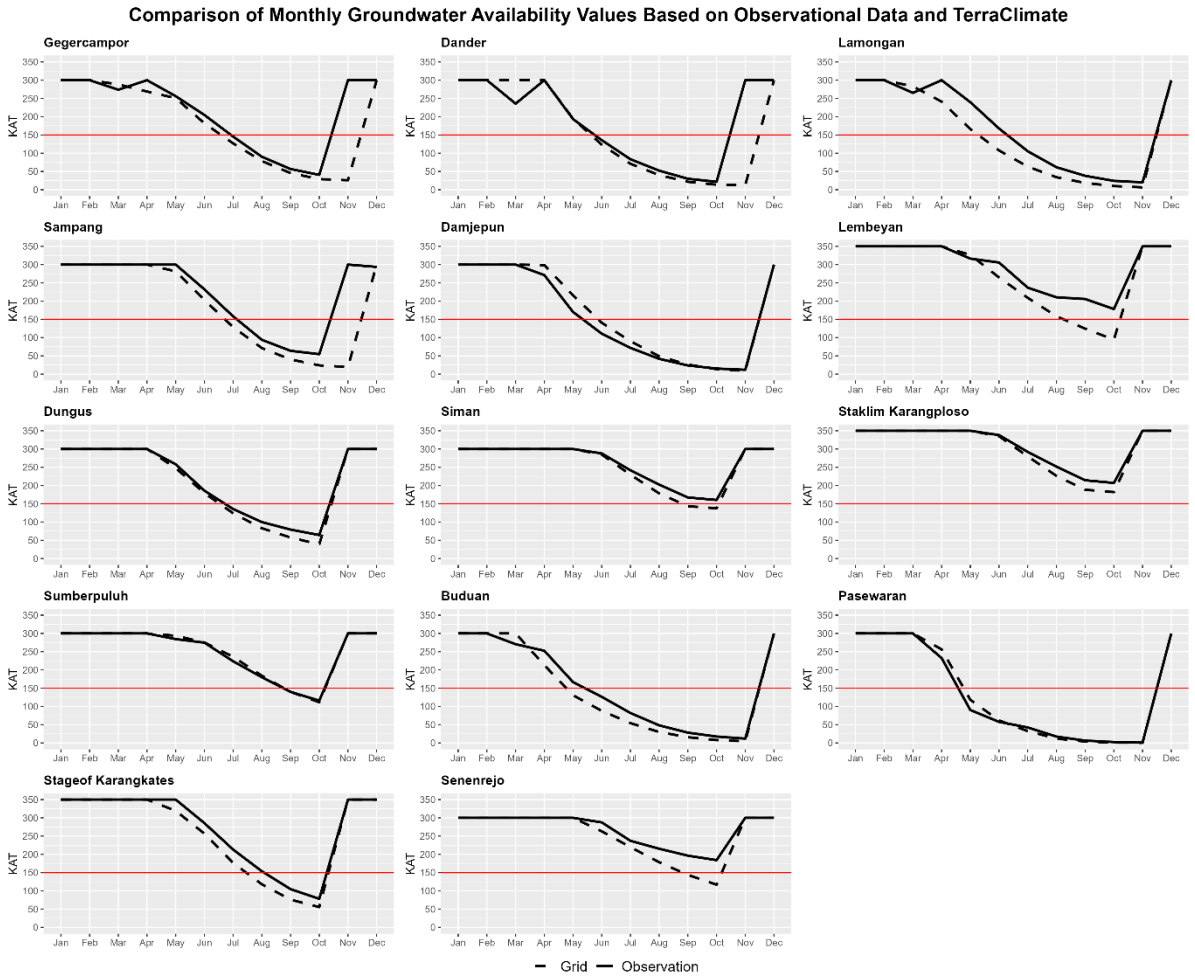

Figure A2. Comparison of Monthly Groundwater Availability Values Based on Observational Data and TerraClimate